PNL-10723
UC-510

Solid-Phase Characterization in Flammable-Gas-Tank Sludges by Electron Microscopy

J. Liu
L. R. Pederson
L. Q. Wang

August 1995

Prepared for the U.S. Department of Energy
under Contract DE-AC06-76RLO 1830

Pacific Northwest Laboratory
Operated for the U.S. Department of Energy
by Battelle Memorial Institute

Battelle

PNL-10723

DISCLAIMER

PACIFIC NORTHWEST LABORATORY
operated by
BATTELLE MEMORIAL INSTITUTE
for the
UNITED STATES DEPARTMENT OF ENERGY
under Contract DE-AC06-76RLO 1830

Printed in the United States of America

Available to DOE and DOE contractors from the Office of Scientific and Technical Information, P.O. Box 62, Oak Ridge, TN 37831; prices available from (615) 576-8401. FTS 626-8401.

Available to the public from the National Technical Information Service, U.S. Department of Commerce, 5285 Port Royal Rd., Springfield, VA 22161.

DISCLAIMER

Portions of this document may be illegible in electronic image products. Images are produced from the best available original document.

PNL-10723
UC-510

Solid-Phase Characterization in Flammable-Gas-Tank Sludges by Electron Microscopy

J. Liu
L. R. Pederson
L. Q. Qang

September 1995

Prepared for
the U.S. Department of Energy
under Contract DE-AC06-76RLO 1830

Pacific Northwest Laboratory
Richland, Washington 99352

Abstract

The crystallinity, morphology, chemical composition, and crystalline phases of several Tank 241-SY-101 (hereinafter referred to as SY-101) and Tank 241-SY-103 (hereinafter referred to as SY-103) solid samples were studied by transmission electron microscopy (TEM), electron energy dispersive spectroscopy (EDS), and electron diffraction. The main focus is on the identification of aluminum hydroxide thought to be present in these tank samples. Aluminum hydroxide was found in SY-103, but not in SY-101. This difference can be explained by the different OH/Al ratios found in the two tank samples: a high OH/Al ratio in SY-101 favors the formation of sodium aluminate, but a low OH/Al ratio in SY-103 favors aluminum hydroxide. These results were confirmed by a magnetic resonance study on SY-101 and SY-103 simulant. The transition from aluminum hydroxide to sodium aluminate occurs at an OH/Al molar ratio of 3.6. It is believed that the study of $Al(OH)_3$ was not affected by sample preparation because all $Al(OH)_3$ is in the solid form according to the NMR experiments. There is no $Al(OH)_3$ in the liquid. It is, therefore, most likely that the observation of $Al(OH)_3$ is representative of the real sludge sample, and is not affected by drying. Similar conclusions also apply to other insoluble phases such as iron and chromium.

Contents

Figures

Tables

1.0 Introduction

Several important physical properties of the sludge in flammable gas tanks, including the viscosity, surface tension, gas permeability, and solubility, may be strongly affected by characteristics of the solid phases in the sludge (Shaw 1980). It has been suggested that an aluminum hydroxide gel may play an important role in the gas generation and retention properties of these tanks. Previous characterization work has shown that the solids in waste tank sludges consist largely of particles having sizes smaller than 1 μm. The ultrafine particles can be studied by TEM and scanning electron microscopy (SEM) (Liu, Chen, and Thomas 1995). Electron microscopy (Hren, Goldstein, and Joy 1979) can be used to study the morphology of the solid phases with angstrom level resolution. Microprobe and nanoprobe EDS also provides compositional information on a nanometer scale. The crystallinity and the crystalline phases can be directly identified by electron diffraction (selected area diffraction, microdiffraction, convergent beam diffraction, etc.) techniques. Characterization of the solid phases in flammable gas tank sludges has been requested by the Westinghouse Hanford Company (WHC) Flammable Gas Program. The characterization work was performed at the analytical electron microscopy facilities in Pacific Northwest Laboratory's (PNL's)[a] 326 Building. Besides electron microscopy on real sludge samples, nuclear magnetic resonance (NMR) was used to study the aluminum phases in SY-101 and SY-103 simulants. The simulant studies allow a precise control of the chemical compositions and experimental conditions. The characterization can be performed in situ, thereby avoiding possible artifacts from sample preparation, such as drying. Both liquid and solid samples, whether amorphous or crystalline, can be studied. The NMR study provides complementary results to the TEM study on the real samples.

(a) Pacific Northwest Laboratory is operated for the U.S. Department of Energy by Battelle Memorial Institute under Contract DE-AC06-76RLO 1830.

2.0 Objective

The purpose of this work is to characterize the crystallinity, morphology, chemical composition, and crystal structure (phase identity) of the solids in tank sludges. The goals for FY 1995 were:

1) To investigate whether electron microscopy can be used to study the solid phases in SY-101 and SY-103 tanks.

2) To investigate whether $Al(OH)_3$ can be identified.

3) To investigate the difference between SY-101 and SY-103 and to compare the results with tank chemistry.

3.0 Experimental Procedure

Solid samples from SY-101 and SY-103 (non-convective layer) were obtained from the 325 Building, including one SY-101 sample, and five SY-103 samples: 6205 Segment 10, 6207 Segment 11, 6225 Segment 12, 6226 Segment 13, and 6246 Segment 14. The samples were dried in the 325 Building Laboratory at 80°C. For SY-103, a large segment number corresponds to the sample near the bottom of the tank, and a small segment number corresponds to the sample near the top of the nonconvective layer. Another homogenized SY-103 sample was obtained from the Pretreatment Program.

The TEM samples were prepared by dispersing a small amount of solid sample (about 1 mg) in methanol solution (< 5 ml), a drop of which was then placed on TEM copper grids covered with carbon films. This work was performed on JEOL 1200 analytical TEM in Laboratory 25 A of the 326 Building, at 120 kV. The analysis then proceeded as follows: 1) the morphology, distribution, and sizes of particles were evaluated by electron imaging; 2) the chemical compositions of the particles were identified by EDS; 3) the crystal structures of the particles were studied by electron diffraction; and 4) the diffraction patterns were compared with the JCPS-EDD™ Data Base published by the International Center for Diffraction Data.

Because sample preparation and drying is a concern, simulant samples were prepared and studied by magnetic resonance technique. The simulant studies do not involve drying, and can provide insight into the behavior of real tank samples. The simulant samples were prepared according to the procedure described by Bryan and Pederson (1994). The samples were prepared using different OH/Al ratios, and were kept at 80°C for two days. Next, the suspensions were centrifuged at 15,000 rpm on a Beckman L2-65B Ultracentrifuge. The samples were loaded into 7-mm Zirconia PENCIL™ rotors. All NMR experiments were performed on both the liquid (supernant) and the solids (sediments) with a Chemagnetic Spectrometer™ (300 MHz - 89 mm wide bore Oxford magnet).

For tank sludge characterization, sample control and sample preparation is critical. The history of the sample should be well documented and traceable; the sample should be representative of the whole tank sludge; and the sample preparation should be performed under well controlled conditions, i.e., the water content and the appearance of the sample should also be accurately recorded. Due to building closure and the difficulty in obtaining the sample, the FY 1995 objective was limited to exploratory and preliminary investigations on samples made available in the 325 Building within the constraints of time and funds. No effort was made to estimate solid content in the samples during the experiment. The FY 1996 work will include traceable samples prepared under well controlled conditions. The history of the SY-101 sample was not completely known to the authors at the time of the work, but the two batches of SY-103 samples are traceable.

Even though imperfect, the current sampling technique produced relevant results:

1) It is believed that the study of $Al(OH)_3$ will not be affected by sample preparation because all $Al(OH)_3$ is in the solid form according to the NMR experiments. There is no $Al(OH)_3$ in the liquid. It is therefore most likely that the observation of $Al(OH)_3$ is representative of the real sludge sample, and is not affected by drying. Similar conclusions also apply to other insoluble phases such as iron and chromium.

2) Two separate batches of SY-103 samples were studied; one was shipped by David Cochran, and the other obtained from the Pretreatment Program Group (Brian Rapko and Gregg Lumetta). Similar results were obtained from those studies, providing greater validity to the TEM study.

3) The TEM study of the real sludge is consistent with the phases obtained in simulant samples, which were not dried. The results are also consistent with studies reported in the literature.

4) The morphology and distribution of the soluble phases, such as sodium aluminate, will be strongly affected by the sample preparation. Much additional work, however, needs to be performed under well controlled conditions to provide information on the morphology of these soluble phases.

4.0 Results and Discussions

4.1 Transmission Electron Microscopy (TEM) of SY-101 Samples

Figure 1a shows a typical TEM image of SY-101 sample. This sample consists of needle-like particles from a few μm to larger than 10 μm throughout the sample; it is homogeneously distributed. This morphology is typical of salt crystals dried from solutions. Figure 1b is a higher magnification of the same sample, showing the rough surface of the crystals. The EDS (Figure 2) indicates that the sample consists mostly of sodium, a small amount of aluminum, and a small amount of chlorine and potassium. This indicates that the SY-101 sample is most likely to be made of sodium-rich salt instead of aluminum hydroxide. Figure 3 is a selected area diffraction pattern with typical single crystalline diffraction patterns. This diffraction pattern was identified as sodium hydroxide hydrate ($NaOH.4H_2O$) or sodium nitrate ($Na_2N_2O_3$ H_2O); no other insoluble solid phases have been found in the SY-101 sample. It has been well established that SY-101 contains abundant amounts of sodium nitrate, carbonate, and oxalate. This is consistent with the EDS analysis of the composition with a major sodium peak. However, the absence of the aluminum-rich phase (no major aluminum peak was found in EDS and microprobe EDS throughout the sample) implies that $Al(OH)_3$ is not a major phase, and the aluminum is included in the sodium-rich salt. It can therefore be concluded that aluminum hydroxide is not the major phase in SY-101. It should be pointed out that the morphology of the soluble particles in SY-101 is likely to have been altered by sample preparation. Only the morphology of the sodium-rich phases, however, may have been altered. Therefore, more controlled experiments should be performed on such samples in the future.

4.2 Transmission Electron Microscopy (TEM) of SY-103 Samples

Figure 4a is the TEM image of the homogenized SY-103 sample from the Pretreatment Program. A similar result was obtained from the SY-103, 6205 Segment 10 sample. It consists of fine particles ($< 1\mu$m) and agglomerates ($> 5\mu$m) of fine particles that vary significantly from the morphology of SY-101. The EDS spectrum (Figure 4b) indicates that aluminum is a major element in this sample, and a large amount of sodium and chromium was also found. Other minor elements include Mn, Ca, K, and Fe. The same SY-103 sample was washed in 3M NaOH solution, therby removing a significant amount of aluminum and sodium, but other insoluble species such as Cr and Mn remained. In SY-103 samples, Cr is found to be associated with the aluminum species. In Segment 11, 12, 13, and 14 many other soluble salts, such as nitrate and sulfate, were observed.

Sodium salt was found to be unstable under an electron beam. Figure 5 is the TEM image of the SY-103 sample after it has been exposed for some time. Essentially all the sodium salt escaped from the particles, leaving a porous, aluminum-rich skeleton behind.

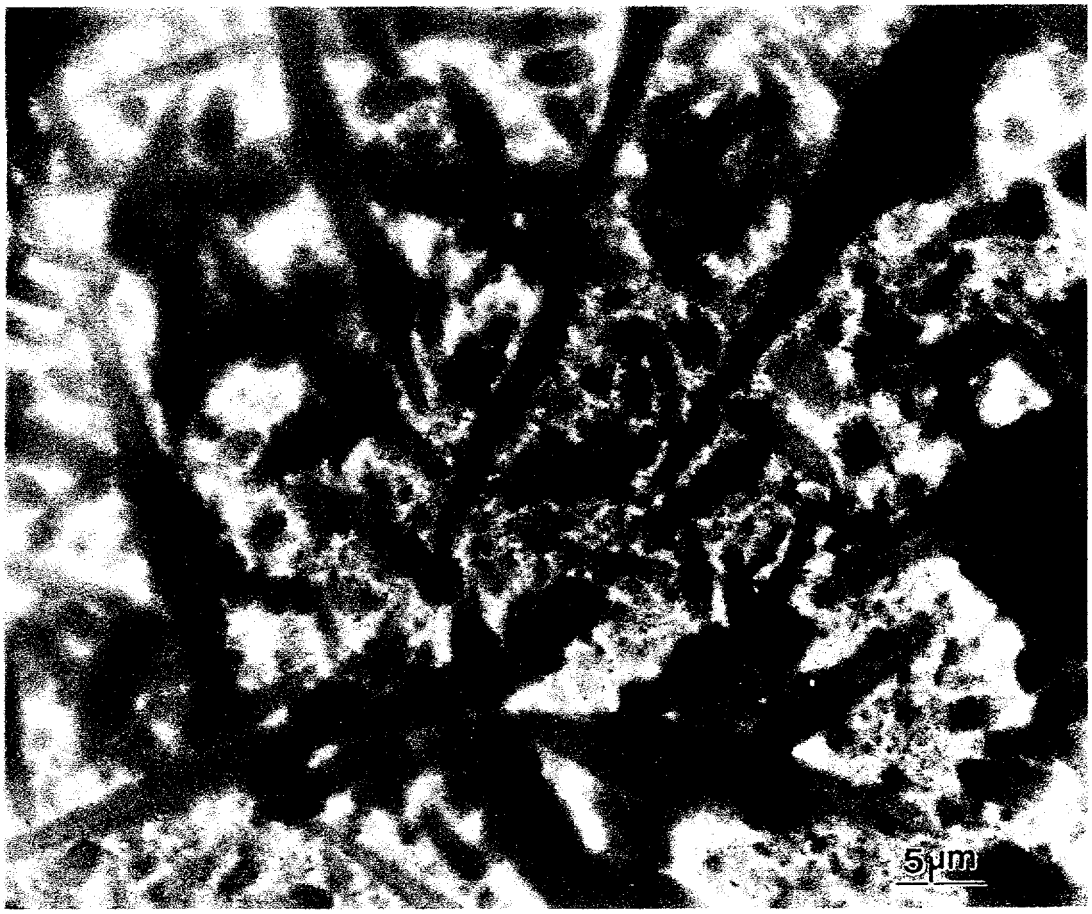

Figure 1a. TEM Image of SY-101 Sample. Needle-like particles larger that 5μm are observed.

Figure 1b. TEM Image of SY-101 Sample under High Magnification. The needle-like shape and rough surface of the particles are typical of dried salts.

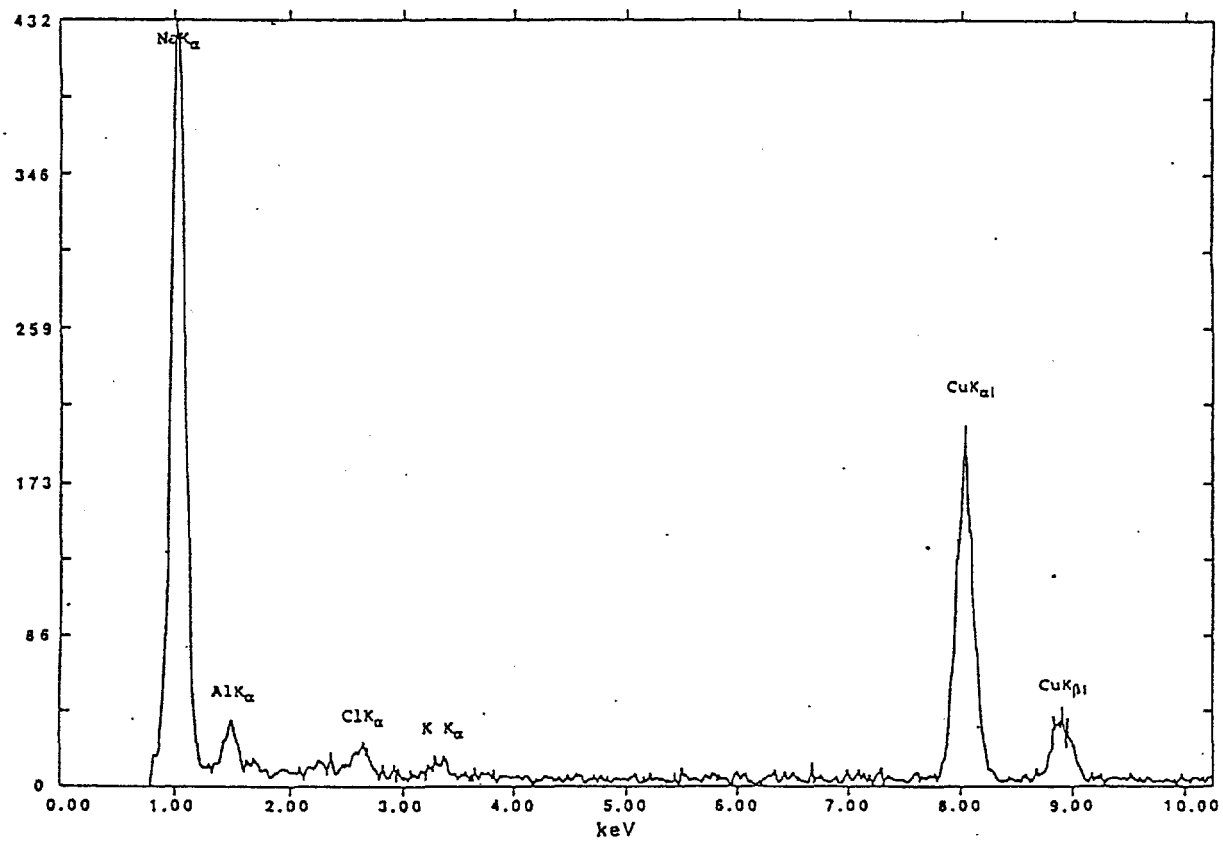

Figure 2. EDS Spectrum of Sodium-Rich Salt in SY-101. Na is the major peak in SY-101. A major aluminum peak is absent throughout the sample.

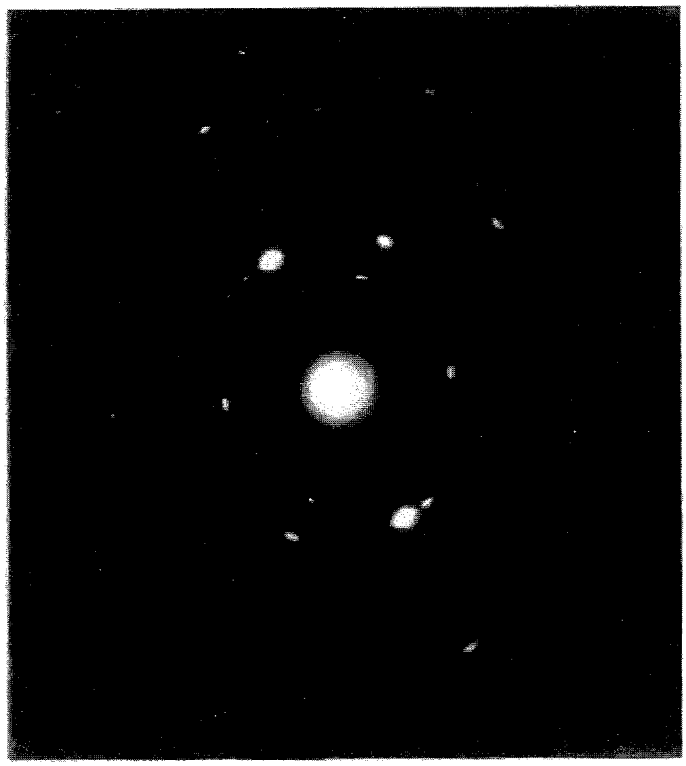

d (Å, measured)	$NaOH.4H_2O$
4.027	4.085
3.377	3.380
3.102	3.160
2.900	2.894
2.578	2.572
2.372	2.440
1.976	2.013
1.525	
1.442	

Figure 3. Typical Selected Area Diffraction with Single Crystalline Diffraction Patterns. This diffraction pattern can be identified as sodium hydroxide hydrate.

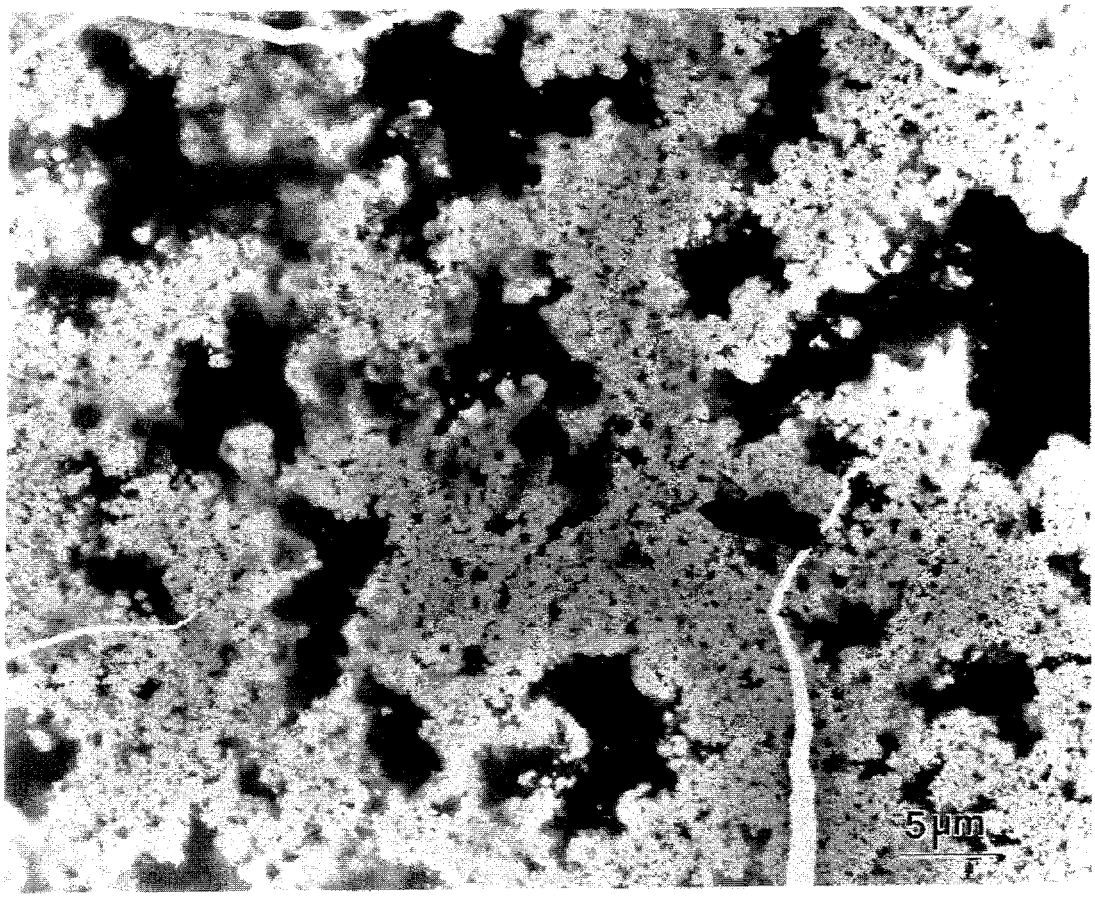

Figure 4a. TEM Image of Homogenized SY-103 Sample. This sample shows agglomerates of nanometer-sized particles. Similar morphology is observed in the Segment 10 sample.

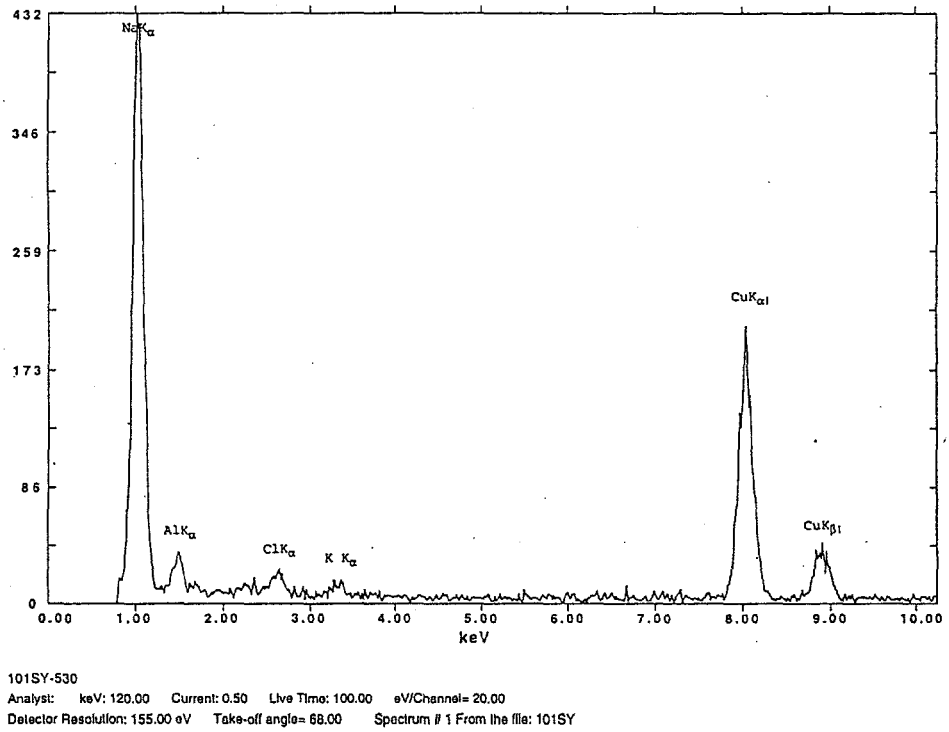

Figure 4b. EDS Spectrum of Aluminum-Rich Phase in SY-103. The major composition in the solid phase is Al, Na, and Cr. After washing in basic solution, some Al and Na are removed, but other elements remain the same.

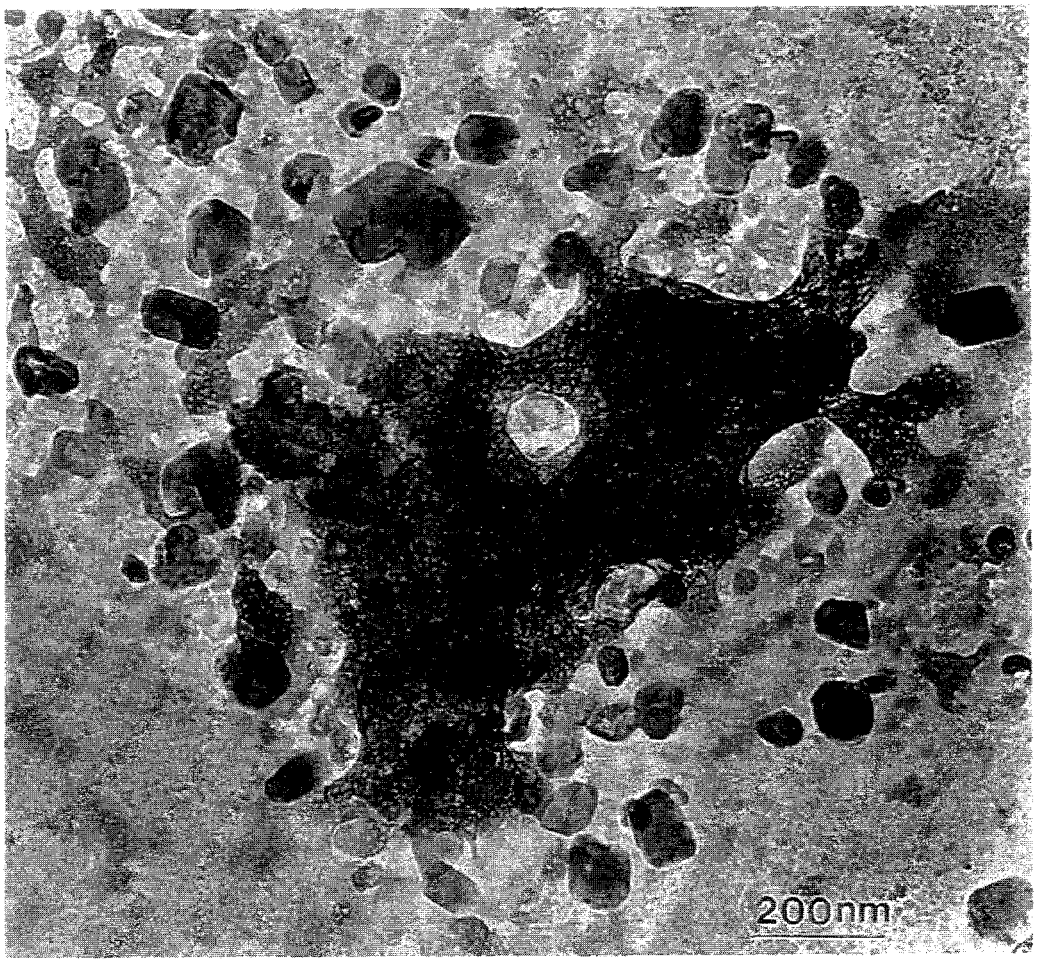

Figure 5. TEM Image of SY-103 Sample After Exposure to Electron Beam. The sodium species is unstable and is removed from the particles during beam exposure, leaving an aluminum-rich skeleton.

Microprobe EDS and microdiffraction suggested that some regions contain particles with aluminum as the most predominant species, as shown in Figure 6. Figures 7a and 7b show the EDS spectrum and the diffraction pattern. The aluminum-rich phase was identified as $Al(OH)_3$.

4.3 Why do SY-101 and SY-103 Vary?

From this study, it can be concluded that aluminum hydroxide is an important phase in SY-103, but not in SY-101. Many other salt crystals, such as nitrate and sulfate, were also found in SY-103 and SY-101 wastes. The difference between SY-103 and SY-101 is interesting, prompting the query as to why aluminum hydroxide is found in SY-103 waste, but not in SY-101 waste. We believe that the

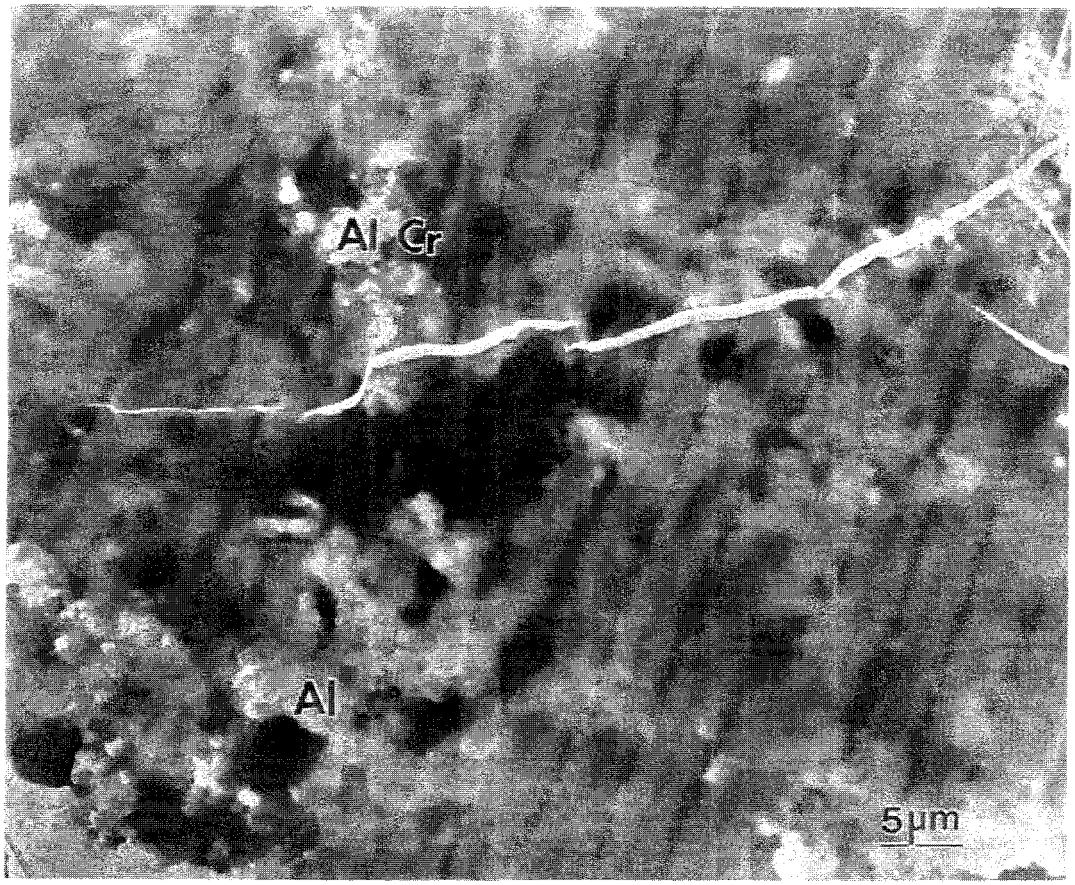

Figure 6. TEM Image of the Aluminum-Rich Particles in SY-103

d (Å, measured)	$Al(OH)_3$
3.982	4.080
2.853	2.890
2.709	2.670
2.404	2.395
1.846	1.900
1.705	1.690

Figure 7. EDS of the Aluminum-Rich Phase in SY-103 and the Corresponding Diffraction Pattern. The aluminum-rich phase can be identified as $Al(OH)_3$. Some chromium is found to associate with aluminum.

difference is caused by the different hydroxide and aluminum concentrations in the two tanks. Tables 1a and 1b list the major cation and anion concentrations in the non-convective layer (1a) and convective layer (1b) (Barton (1995), Van Vleet (1995) and Herting (1992)). The hydroxide-to-aluminum ratio in SY-101 is clearly higher than that found in SY-103. According to Bradley and Hanna (1994), there are several reasons for this variance in aluminum species under basic conditions depending upon the OH/AL ratios: for OH/Al >4.4, tetrahedral aluminum (sodium aluminate) is more stable; for OH/Al < 4.1, octahedral aluminum (aluminum hydroxide precursor) is more stable.

Table 1a. Major Cation and Anion Concentrations in SY-101 and SY-103 Sludge (Non Convective Layer)

Analysis	SY-101 Comp.3 Bulk	SY-103 Seg. 10 -14 Comp.
Density g/ml	1.7	1.57
TOC, wt%	2.00	1.06
TIC, wt%	0.88	0.88
Al, wt%	3.39	3.50
Na, wt%	22.0	18.7
Hydroxide, wt%	2.50	1.84
Cr, wt%	0.645	0.66
Nitrite, wt%	9.6	8.19
Nitrate, wt%	11.6	9.81
Iron, wt%	0.040	0.21
Phosphate, wt%	0.83	1.56
Water, wt%	31.0	33
Hydroxide, M	2.5	1.7

Table 1b. Major Cation and Anion Concentrations in SY-101 and SY-103 Sludge (Convective Layer)

Analysis	SY-101Comp. 1 Liquid	SY-103 Seg. 2-7 Liquid
Density g/ml	1.49 - 1.57	1.47
TOC, wt%	0.97	0.66
TIC, wt%	0.11	-
Al, wt%	3.12	2.81
Na, wt%	18.00	14.39
Hydroxide, wt%	2.68	1.95
Cr, wt%	0.01	0.002
Nitrite, wt%	10.8	9.73
Nitrate, wt%	10.4	12.18
Iron, wt%	0.003	< 0.0021
Phosphate, wt%	0.35	0.21
Water, wt%	42	48.4
Hydroxide, M	2.41	1.69

The solubility diagrams of aluminum hydroxide by Barney (1976) provide some clues about the behavior of the aluminum species in the two tanks (Figure 8). The solubility of aluminum hydroxide increases rapidly with hydroxide concentration at about 0.5 M NaOH and reaches a maximum at 1.6 M NaOH. With more NaOH, sodium aluminate becomes more stable and the solubility of sodium aluminate gradually decreases with increasing NaOH concentration. When the compositions of the SY-101 and SY-103 were plotted on the solubility diagram, it was found that all the data from SY-101 (circles) fell under the sodium aluminum solubility line. The data (squares) from SY-103, however, clustered around the solubility line of aluminum hydroxide, with some data points above the solubility line of aluminum hydroxide. This implies that the aluminum in SY-103 can precipitate as aluminum hydroxide, but is less likely to occur in SY-101.

The TEM results foster some implications about the behavior of SY-101 and SY-103 tanks. Because SY-101 composition falls under the solubility line of sodium aluminate, the flammable gas generation and retention will not necessarily be by adding more hydroxide to the tank. On the sodium aluminate side, the addition of hydroxide will not dissolve the solid phase. Instead, it will reduce the

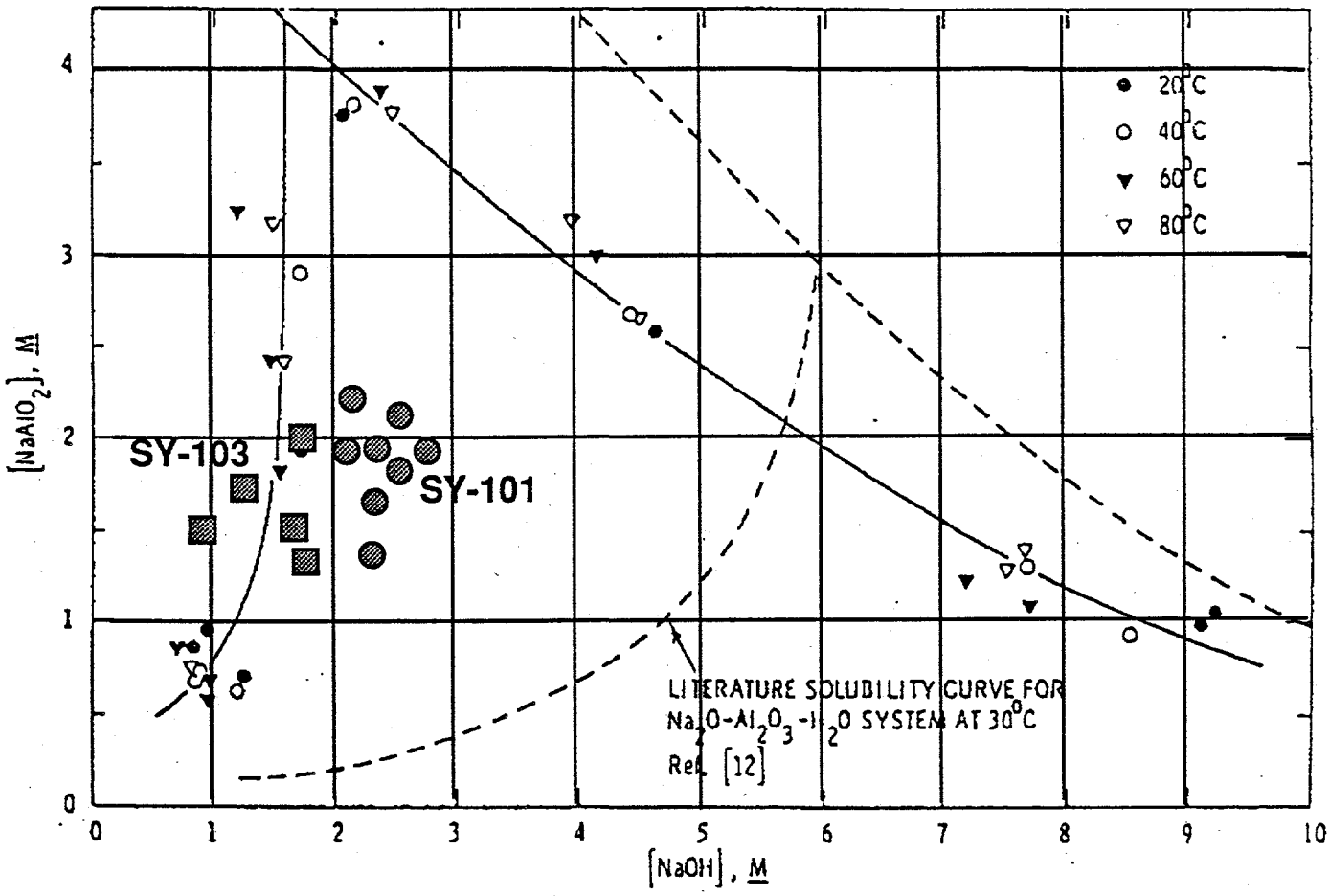

Figure 8. Solubility Diagram of Aluminum Hydroxide (S. S. Barney, ARH-ST-133, 1976, and B. Barton, 1995). All SY-101 data fall under the solubility line of sodium aluminate, and the SY-103 data are near the solubility line of $Al(OH)_3$.

solubility of the solid phases. A comparison of the composition of the two tanks also implies that SY-103 should have a more serious problem than SY-101 if $Al(OH)_3$ were responsible for the flammable gas issue.

To quantitatively study aluminum hydroxide's solubility and stability under well-controlled conditions, simulant samples were prepared according to procedures described in Bryan and Pederson (1994). Because this study does not require the drying of the samples, it can provide insights into the behavior of the aluminum species in high electrolyte concentrations. Table 2 lists applicable concentrations of SY1-SIM-93B using aluminum nitrate as the precursor, and Table 3 lists applicable concentrations of SY1-SIM-92A using sodium aluminate as the precursor. In these experiments the

Table 2. Concentrations of Components in SY1-SIM-93B

Component	M (mole/L)	Wt%
Na_3HEDTA	0.21	6.04
$Al(NO_3)_3$ 9H2O	0.43	12.49
$NaNO_2$	2.0	10.69
$NaNO_3$	0.4	2.63
Na2CO3	0.2	1.64
NaOH	3.4	10.53
H_2O		55.98
Total		100

Table 3. Concentrations of Components in SY1-SIM-92A

Component	M (mole/L)	Wt%
Na3HEDTA	0.205	4.99
NaCl	0.526	1.97
Na3PO4 12H2O	0.179	4.36
NaNO2	3.95	17.45
NaNO3	2.2	11.97
Na2CO3	0.4	2.71
NaF	0.1	0.27
Na2SO4	0.032	0.29
CaCl2	0.0083	0.06
KCl	0.146	0.7
Cr(NO3)3 9H2O	0.1051	2.69
Cu(NO3)2 2.5H2O	0.0002	0.0
Fe(NO3)3 9H2O	0.0074	0.19
Ni(NO3)2 6H2O	0.0021	0.04
NaOH	2.45	6.28
NaAlO2 0.21NaOH 1.33H2O	2.05	15.1
H2O		30.93
Total		100.0

aluminum concentration was kept constant, and the sodium hydroxide concentration was varied. The samples were aged for two days at 80°C. The relative concentration of hydroxide was changed over a wide range; the samples were then studied using NMR.

These NMR results are summarized in Figures 9a and 9b. The peak at 80 ppm comes from the tetrahedral aluminum (sodium aluminate) and the peak 4 ppm comes from the octahedral aluminum (hydroxide). The peak shape (the broadness and the side bands) is related to the mobility (chemical homogeneity) of the atoms in the sample and sample spinning in the experiments. A homogeneous chemical environment will produce a sharp peak, and a solid sample will produce a broad peak. The side bands come from the magic angle spinning for the NMR experiments. In SY1-SIM-93B, and at OH/Al = 3.60 and above, all aluminum is soluble as tetrahedral aluminum (sodium aluminate). No solid phase is found. Below OH/Al = 3.60, soluble sodium aluminate and solid phase aluminum hydroxide coexists, and below OH/Al $<$ 1.83, all aluminum exists as insoluble aluminum hydroxide. No aluminum species is found in the liquid. These conclusions are consistent with the behavior in both the real tank samples and with the literature (Bradley and Hanna 1994). If the NMR data were plotted in the Barney diagram, the same trend would be observed, except that the precipitation of aluminum hydroxide occurred at a higher concentration than predicted by the solubility diagram. Therefore, the current NMR data falls between the Barney solubility lines and the literature solubility lines for Na_2O-Al_2O_3-H_2O.

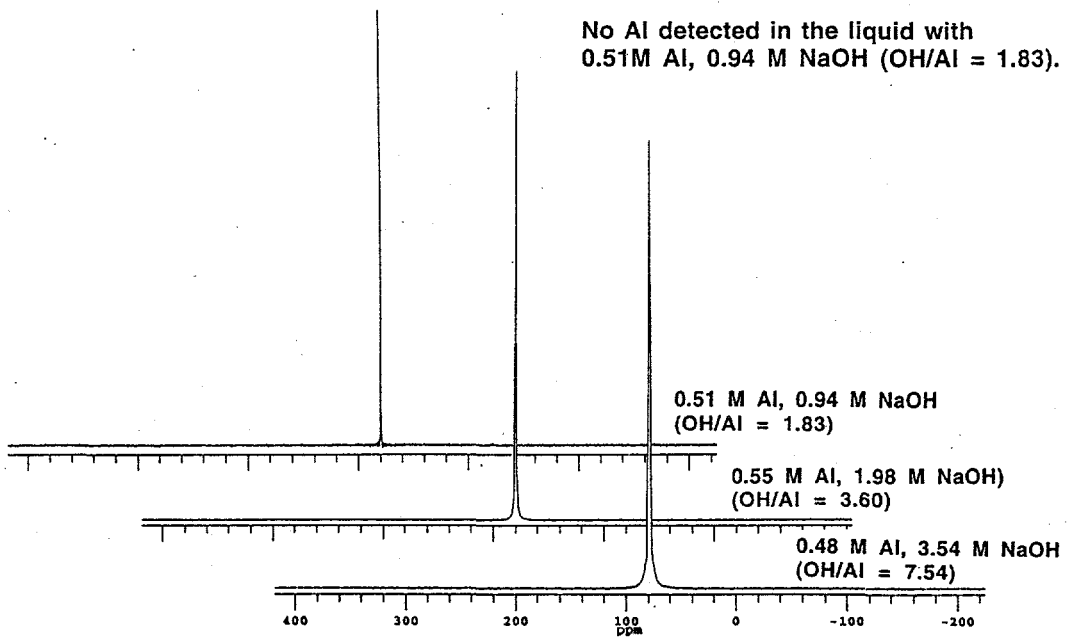

Figure 9a. NMR Spectra of Tetrahedral Aluminum (80 ppm) in the Liquid Phase of SY-1-SIM-93B Simulant with Different OH/Al Ratio

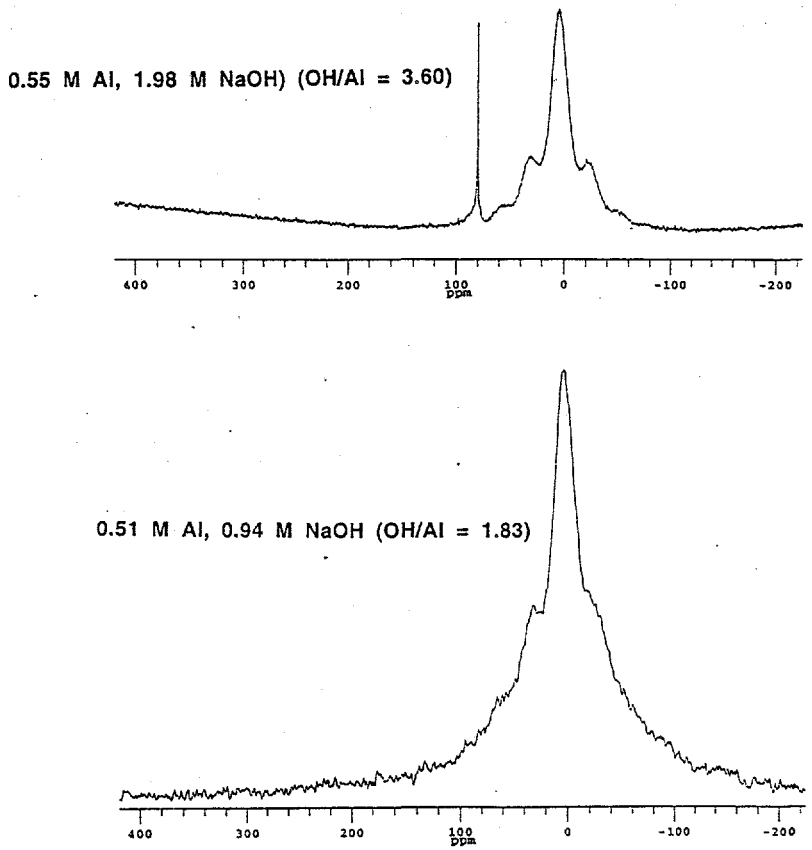

Figure 9b. NMR Spectra of Octahedral Aluminum Hydroxide Precipitated at Low OH/Al Ratio. $Al(OH)_3$ (4 ppm) begins to precipitate as solid particles at 1.98 M NaOH concentration. All aluminum species precipitate as $Al(OH)_3$ at 0.94 M NaOH concentration.

For SY1-SIM-92A, because the starting material is already sodium aluminate, only tetrahedral aluminum was found regardless of the hydroxide concentration (Figure 10).

Another observation is that the NMR peaks are quite broad in Figures 9 and 10 for high hydroxide concentrations. This suggests that at high hydroxide concentrations the sodium aluminate exists as molecular clusters, rather than real solution species. As discussed in previous sections, a broad peak is indicative of the inhomogeneous chemical environment in solid particles.

All the NMR results are summarized in Table 4. Because the phase behavior of aluminum hydroxide under basic conditions is still a poorly studied subject, especially with high background electrolyte, this study did not intend to provide an accurate boundary and a complete phase diagram. There are also different ways to present and interpret the results. However, the use of the NMR technique provided some insight into the chemistry of the real samples. This study indicated that the

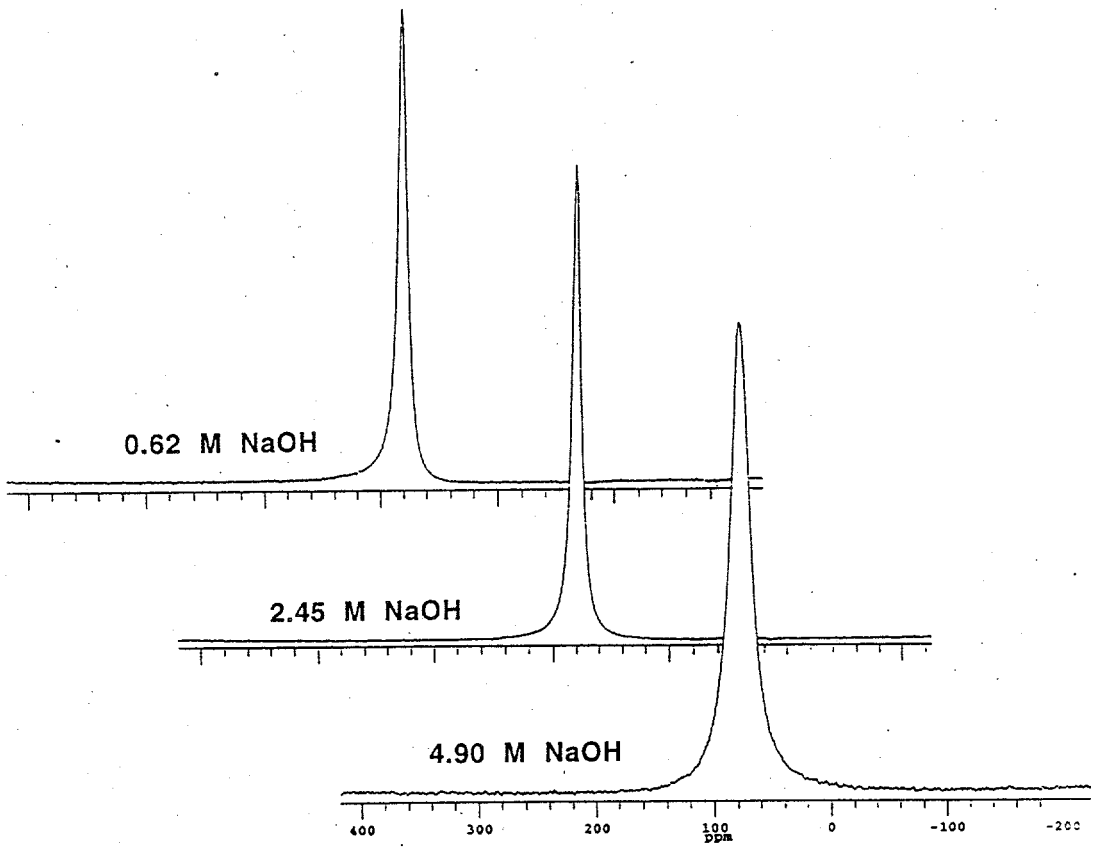

Figure 10. Only Tetrahedral Aluminum is Found by NMR in SY1-SIM-92A Simulant. The starting material in these samples is sodium aluminate, which contains sodium hydroxide. The aluminum species in sodium aluminate is already in the tetrahedral form, and it will not be changed within the compositional range explored in this study. The peak broadens at high hydroxide concentration, indicating the aluminum species in the solution begins to aggregate and cluster.

Table 4. Aluminum Speciation According to NMR Study

OH (total) /Al	Phases
< 1.83	Aluminum hydroxide solid, no Al in liquid
1.83 - 3.60	Aluminum hydroxide solid, sodium aluminate liquid
3.60 - 7.54	Sodium aluminate liquid
> 7.54	Sodium aluminate clusters

transition from aluminum hydroxide to sodium aluminate occurs at OH/Al 3.6 (about 2 M NaOH); this number is consistent with the latest literature data (Bradley 1994) for pure aluminum hydroxide; it lies between the Barney diagram and the Bradley 1994 results. The same trend is observed in the tank waste samples: a low hydroxide concentration in SY-103 favors the formation of aluminum hydroxide. The NMR results also imply that the TEM results on $Al(OH)_3$ are reliable even though the TEM work involves drying the sample. Because the solution in the two tank samples contains a high concentration of soluble species, including aluminum, it is generally accepted that some soluble species will precipitate from the solution. Therefore, not all the solid phases observed in the TEM study represent real solid phases in the samples before drying. The NMR study on simulant samples indicates that all $Al(OH)_3$ should be in the solid phase, and no soluble $Al(OH)_3$ should be in the liquid phase. We conclude that the solid $Al(OH)_3$ observed in TEM is real, and is not produced by precipitation during drying.

5.0 Summary

The crystallinity, morphology, chemical composition, and crystalline phase of several SY-101 and SY-103 solid samples were studied by TEM, EDS, and electron diffraction. The main focus of the preliminary investigation in FY 1995 was on the identification of aluminum hydroxide thought to be present in these tank samples. The results were compared with NMR studies conducted on SY-101 and SY-103 simulants.

- Aluminum hydroxide is observed in SY-103. Other soluble nitrate and sulfate phases are also observed in SY-103.

- Both sodium and aluminum salts are observed in SY-101. No aluminum hydroxide is observed in SY-101.

- The study of $Al(OH)_3$ is consistent with the tank chemistry. SY-101 composition falls under the solubility lines of sodium aluminate, and SY-103 composition is near the solubility line of $Al(OH)_3$. Therefore it is expected that $Al(OH)_3$ can precipitate in SY-103.

- NMR experiments suggest that aluminum hydroxide will precipitate at low hydroxide concentration, and sodium aluminate will form for a higher OH/Al ratio.

- Within the experimental range, all soluble aluminum is tetrahedral (aluminate). All $Al(OH)_3$ is in the solid phase, and no $Al(OH)_3$ is observed in the liquid phase. This suggests that drying the sample is unlikely to cause precipitation of $Al(OH)_3$ and, therefore, the TEM study of $Al(OH)_3$ is reliable.

- All the soluble aluminate exists as sodium aluminate. The narrow peak at a lower hydroxide suggests that the aluminum is truly a soluble species, but the broader peak at high hydroxide concentrations suggests that the aluminum species begins to aggregate into clusters and ultrafine colloidal particles.

- The TEM study on tank samples and the NMR study on simulants is consistent with reported literature results.

- Insoluble solid phases containing Cr, Fe, and Mn are observed in SY-103; they are not affected by washing.

This report contains only the results of preliminary studies. The solubility, stability, and morphology of the aluminum-rich phases in SY-101 and SY-103 should be studied under a variety of controlled experimental conditions. The morphology and distribution of the soluble phases such as sodium aluminate will be strongly affected by the sample preparation. Much work needs to be done under well controlled conditions to provide information on the morphology of these soluble phases.

6.0 References

Barney, S. S. 1976. *Vapor-Liquid-Solid Phase Equilibrium of Radioactive Sodium Salt Wastes at Hanford*. ARH-ST-133, Atlantic Richfield Hanford Company, Richland, Washington.

Bradley, S. M., and J. V. Hanna. 1994. "^{27}Al and ^{23}Na MAS NMR and Powder X-Ray Diffraction Studies on Sodium Aluminate Speciation and the Mechanistic of Aluminum Hydroxide Precipitation upon Acid Hydrolysis." *J. Am. Chem. Soc.* 116:7771-7783.

Bryan, S.A., and L. R. Pederson. 1994. *Composition, Preparation, and Gas Generation Results from Simulated Wastes of Tank 241-SY-101*. PNL-10075, Pacific Northwest Laboratory, Richland, Washington.

Barton, B. 1995. *103-SY Core Sample and Gas Monitoring Results*, presentation at Chemical Reaction Sub-Tank Advisory Panel Meeting, August 30, 1995, Richland, Washington.

Herting, D. L. 1992. *Laboratory Characterization of Samples Taken from Hanford Waste Tank 241-SY-101*. WHC-SD-DTR-024, Westinghouse Hanford Company, Richland, Washington.

Hren, J. J., J. I. Goldstein, and D. C. Joy. 1979. *Introduction to Analytical Electron Microscopy*. Plenum Press, New York.

Liu, J., Y. L. Chen, and L. E. Thomas. 1995. *Third Quarter Report for Tank Waste Treatment Science*. TWRSPP-95-019, Pacific Northwest Laboratory, Richland, Washington.

Shaw, D. J. 1980. *Introduction to Colloidal and Surface Chemistry*. Butterworth, Inc., Boston, Massachusetts.

Van Vleet, R. J. 1993. *Radionuclide and Chemical Inventories for the Double-Shell Tanks*. WHC-SD-TI-543, Westinghouse Hanford Company, Richland, Washington.

Distribution

No. of Copies

OFFSITE

S. Agnew
Los Alamos National Laboratory
MS-C345, Group INC-4
P.O. Box 1664
Los Alamos, NM 87545

E. K. Barefield
225 North Avenue
Boggs Chemistry Building
Georgia Institute of Technology
Atlanta, GA 30332

Westinghouse Savannah River
P.O. Box 616
Aiken, SC 29802
Attn: N. E. Bibler, Bldg. 773A, Rm 108
P. d'Entremont, Bldg. 703-H

U.S. Department of Energy
Trevion II
Washington, DC 20585-0002
Attn: P. Bryns, EM-35
C. O'Dell, EM-36
D. Pepson, EM 36

D. O. Campbell, MS 6268
Oak Ridge National Laboratory
P.O. Box 2008
Oak Ridge, TN 37831-6268

SAIC
20300 Century Blvd.
Germantown, MD 20874
Attn: R. Daniels
P. Hogroian

B. S. Hudson
Lawrence Livermore National Laboratory
P.O. Box 271
Lindsborg, KA 67456

No. of Copies

L. Kovach
NUCON
P.O. Box 29151
Columbus, OH 43229

Argonne National Laboratory
9700 South Cass Avenue
Argonne, IL 60439
Attn: D. Meisel
L. Stock, Chemistry Division

W. W. Schulz
727 Sweetleaf Drive
Wilmington, DE 19808

ONSITE

6 **DOE Richland Operations Office**

R. F. Christensen	S7-54
R. E. Gerton	S7-54
J. M. Gray	S7-54
M. F. Jarvis	S7-54
G. Rosenwald	S7-54
Reading Room	A1-65

20 **Westinghouse Hanford Company**

H. Babad	S7-30
W. B. Barton	R2-11
R. J. Cash	S7-15
K. A. Gasper	G3-21
D. L. Herting	T6-09
J. D. Hopkins	R2-11
J. Jewett	T6-09
G. D. Johnson (3)	S7-15
N. W. Kirch	R2-11
J. W. Lentsch	S7-15
R. M. Marusich	H5-65
N. G. McDuffie	S7-15
D. M. Ogden	H0-34

No. of Copies		
	M. A. Payne	S7-14
	J. C. Person	T6-09
	D. A. Reynolds	R2-11
	D. J. Sherwood	S7-15
	R. J. Van Vleet	H4-63
54	**Pacific Northwest Laboratory**	
	Z. I. Antoniak	K7-15
	J. L. Bates	K2-45
	J. W. Brothers (5)	K5-22
	S. A. Bryan	P7-25
	L. L. Burger	P7-25
	D. M. Camaioni	K2-38
	J. A. Campbell	P8-08
	P. A. Gauglitz	P7-41
	S. C. Goheen	P8-08
	R. J. Hall	K8-28
	R. T. Hallen	P8-38
	J. D. Hudson	K7-15
	M. A. Lilga	P8-38
	J. D. Norton (10)	K2-44
	L. R. Pederson (10)	K2-44
	H. C. Reid	K7-15
	W. D. Samuels	K2-44
	R. D. Scheele	P7-25
	G. F. Schiefelbein	P8-38
	A. Shekarriz	K7-15
	C. W. Stewart	K7-15
	R. W. Stromatt	P7-22
	J. M. Tingey	P7-25
	D. S. Trent	K7-15
	H. H. Van Tuyl	P7-22
	Information Release Office (7)	K1-06